Available online at www.sciencedirect.com
ScienceDirect
Building and Environment 42 (2007) 3529–3539
BUILDING AND ENVIRONMENT
www.elsevier.com/locate/buildenv

Study of PV-Trombe wall assisted with DC fan

Ji Jie*, Yi Hua, Pei Gang, Jiang Bin, He Wei

Department of Thermal Science and Energy Engineering, University of Science and Technology of China, Hefei, China

Received 7 April 2006; received in revised form 3 August 2006; accepted 24 October 2006

Abstract

A novel PV-Trombe wall (PV-TW) assisted with DC fan is presented in this paper. Based on the original PV-TW model, theoretical simulations have been conducted for PV-TW with and without assisted DC fan. At the same time, field tests for these two cases have been performed to validate the model, and then the simulated and experimental results are found in considerably good agreement after their comparisons. A significant temperature increase of indoor temperature with a maximum of 14.42 °C, if compared with the reference room, can be obtained by the PV-TW assisted with a relatively small DC fan by testing. Meanwhile, the experimental average electrical efficiency of the PV-TW assisted with DC fan can reach 10–11%, due to the glass cover. Furthermore, the testing results for PV-TW assisted with DC fan show that the average (during 7:00–17:00) temperature of PV cells reduces by 1.28 °C and the average indoor temperature increases by 0.50 °C, if compared with the original PV-TW with similar solar radiation, and more than one degree lower ambient temperature. It indicates that the assisted DC fan can help improving the indoor temperature and cooling the PV cells in some measure. The potential of PV-TW can be exerted by the assisted DC fan.

Keywords: PV-Trombe wall; DC fan; Simulated and experimental results; Comparison

1. Introduction

Since the past decades, Trombe wall has received considerable attention for space heating as an effective means of using solar energy. It is simple, economical and suitable to a wide range of latitudes, but its less function and unaesthetic property have limited its spread so much that it needs to be improved. Consequently, some improvements for different latitudes have been carried out [1–5], but all of them are thermal applications. Otherwise, when solar electrical power generation is considered, building integrated photovoltaics (BIPV) has so many significant advantages and it is advocated worldwide [6]. In order to integrate them together and exert their own advantages, a new concept of Trombe wall design named "PV-Trombe wall" (PV-TW) for both space heating and cooling PV modules has been presented in our former publication [7]. It not only generates electricity, but also provides space heating; meanwhile it brings more aesthetic value. The model of PV-TW and theoretical investigation of PV-TW's thermal and electrical performance have been reported in [7], but the experimental study has not been dealt with yet.

Nevertheless, it is found that the cooling of the PV cells was not adequate so that the solar energy captured by the PV glass panel was not given the best out of. Since the natural convection induced by the original PV-TW was insufficient, a forced convection introduced by DC fan was considered. So far, there were some researches about DC fan applied on PV systems. For instance, DC fan was applied on a roof solar collector [8,9], a PV slat window [10], a solar chimney [11] and a thermoelectric roof solar collector [12,13] in Thailand. However, all of them, no matter experimental or theoretical, were concerned about cooling or ventilation because they were developed in the hot and humid Thailand, while it is not the case in most part of China like Hefei. In addition, little attention was paid on how DC fan improves the system's performance.

As we know, the electricity generated by PV cells is solar radiation proportional. In our consideration, because the PV cells' temperatures are higher at a better solar radiation, the requirement of cooling the PV cells is much

*Corresponding author. Tel.: +86 551 3601652; fax: +86 551 3601652.
E-mail address: jijie@ustc.edu.cn (J. Jie).

0360-1323/$ - see front matter © 2006 Elsevier Ltd. All rights reserved.
doi:10.1016/j.buildenv.2006.10.038

Nomenclature

A_j surface area exposed to the interlayer (m^2)
A_S cross-sectional area normal to the height direction of the air duct (m^2)
A_V area of the winter air vent (m^2)
C_{in}, C_{out} loss coefficients at top and bottom winter air vent, respectively
C_f fraction factor along the air duct
C_p, C_w, C_G specific heat capacity of air, wall and glass, respectively (J/kg K)
d air duct hydraulic diameter (m)
D, D_w, D_G depth of air duct, the thickness of the wall and glass panel (m)
E electric power rate generated by PV cells (W/m^2)
g gravitational acceleration, $g = 9.80665(m/s^2)$
G total solar radiation on the vertical plane (W/m^2)
G_{pv} solar radiation which arrives on the PV surface (W/m^2)
h_{co}, h_{ci} convection heat transfer coefficients on the outside surface and inside surface of PV glass panel (W/m^2K)
h_{ro}, h_{ri} radiation heat transfer coefficients on out side surface and inside surface of PV glass panel (W/m^2K)
h_{wo}, h_{wi} convection heat transfer coefficients on the outside surface and the inside surface of PV-TW wall, respectively (W/m^2K)
h_{rwo} radiation heat transfer coefficient on the outside surface of PV-TW wall (W/m^2K)
h_{nrwo} radiation heat transfer coefficient on the outside surface of normal wall (W/m^2K)
h_{nwi}, h_{nwo} convection heat transfer coefficient on the inside and outside surface of normal wall, respectively (W/m^2K)
$K_{\tau\alpha}$ a modified coefficient of transmissivity
L height of PV-TW (m)
L_{room} depth of room (m)
$\dot{m}$ ventilated mass flow rate (kg/s)
ΔP pressure head provided by DC fan (P_a)
P_f power of DC fan (W)
R_{Trombe} ratio between the area of PV-TW wall and the total southern wall area
T_p, T_e, T_a temperatures of PV glass panel, ambient, the air in the duct, respectively (°C)
T_{wo}, T_{wi} temperatures of outside and inside surface of PV-TW wall (°C)
T_w temperatures of PV-TW wall (°C)
T_{nwo}, T_{nwi} temperatures of outside and inside surface of normal wall (°C)
T_{out}, T_{in} temperatures of top and bottom winter air vent (°C)
T_r indoor temperature of the PV-TW room (°C)
T_j air temperature in the air interlayer (°C)
U_j overall heat transfer coefficient between interlayer and indoor room (W/m^2K)
V_a velocity of the airflow in the duct (m/s)
w width of PV-TW (m)
w_{room} width of the PV-TW room (m)

Greek symbols

α_{PV}, α_{nwall}, α_{wall} absorptivity of the PV cells, the normal wall, PV-TW wall, respectively
α_{WPV}, α_{NPV} equivalent absorptivities of the elements with and without PV cell on the glass panel, respectively
τ_{PV}, τ transmissivity of the PV cells' outside layers, the elements without PV cell on the glass panel, respectively
β heat expansion coefficient (K^{-1})
ε ratio of PV cell coverage
η_0 electrical efficiency at standard conditions
θ incident angle
ρ, ρ_G, ρ_w density of the air, glass, wall, respectively (kg/m^3)
ξ_1, ξ_2, ξ_3 emissivity factors
λ_a, λ_G, λ_w thermal conductivity of air, glass, wall, respectively (W/m K)

more, and the DC fan, which is installed in the air duct and driven by solar radiation proportional direct current, can satisfy it well. Besides, the requirement of cooling and the operation of DC fan can couple together natively without any controlling management. Furthermore, DC fan accelerates import of the hot air in the air duct. If PV-TW is periodically used, such as for a diurnal use, the indoor space should be heated in a short-term, and the DC fan can help expediting the process and creating more comfortable thermal environment.

PV-TW systems with and without assisted DC fan are theoretically and experimentally investigated based on the PV-TW's model [7] in this study. The DC fan can be driven by the PV glass panel itself or another separate PV module, and the latter is adopted in our research as a result of the requirement of voltage matching. A relatively small DC fan, whose rated voltage and current are 12 V and 0.45 A respectively, is chosen to fit the size of the PV-TW, and it is driven by another small PV module with a rated power of 10 W_P. This paper, mainly, aims at validating the theoretical model by experiments and investigating the performance of this system such as the electrical generation and indoor temperature rise. The ability of DC fan in improving the performance is also studied by comparing

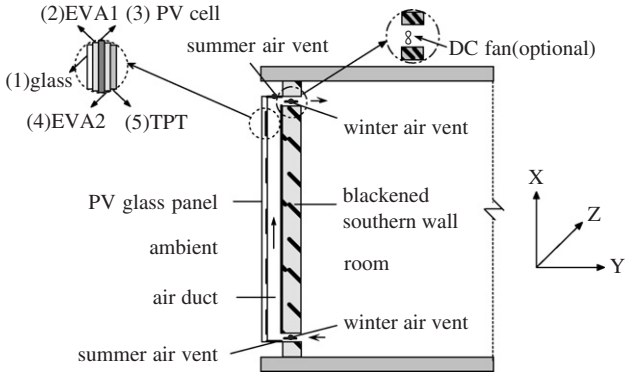

Fig. 1. Schematic diagram of PV-Trombe wall with DC fan for winter heating.

the novel DC fan assisted PV-TW system with the original PV-TW system.

2. Description of the PV-TW system assisted with DC fan

The PV-TW system assisted with DC fan, as shown in Fig. 1, is composed of a PV glass panel on which some PV cells are affixed, a blackened wall acting as a thermal absorber and an air duct in between. There are also two air vents for winter heating and two air vents for summer cooling. In addition, it is noticeable that the PV glass panel consists of five layers.

For winter heating, the winter air vents are periodically opened while the summer air vents are always closed. The system sucks the indoor air from the bottom winter air vent, then vents into the room through the top winter air vent. The airflow in the air duct, which is driven by thermosiphon and an optional DC fan (without or with DC fan), removes heat from both the PV glass panel and the blackened wall. Then, through the top winter air vent, the warmed air is mixed in the room and enters the bottom air vent at last. Undesired reverse airflow during night can be prevented by the periodical open of vents.

3. Mathematic model

The detailed model of PV-TW has been given in our former paper [7], so only the primary equations and significant differences are given below for the PV-TW system assisted with DC fan, and the denotations can be seen in the nomenclature.

3.1. Energy balance of PV glass panel

Since the heat capacity of the flimsy PV cells is neglected, the energy balance can be obtained as follows:

$$\rho_G c_G \frac{\partial T_p}{\partial t} = \frac{\partial}{\partial X}\left(\lambda_G \frac{\partial T_P}{\partial X}\right) + \frac{\partial}{\partial Z}\left(\lambda_G \frac{\partial T_P}{\partial Z}\right) + b, \quad (1)$$

where $b = (S_c + S_p T_p)/D_G$

(1) for the elements with PV cell on the glass panel:

$$S_c = \alpha_{WPV} G - E + h_{co} T_e + \xi_1 h_{ro} T_e + h_{ci} T_a + \xi_2 h_{ri} T_{wo},$$

$$S_P = -(h_{co} + \xi_1 h_{ro} + h_{ci} + \xi_2 h_{ri}),$$

(2) for the elements without PV cell on the glass panel:

$$S_c = \alpha_{NPV} G + h_{co} T_e + \xi_1 h_{ro} T_e + h_{ci} T_a + \xi_2 h_{ri} T_{wo},$$

$$S_P = -(h_{co} + \xi_1 h_{ro} + h_{ci} + \xi_2 h_{ri}),$$

where α_{WPV}, α_{NPV} are the equivalent absorptivities of the elements with and without PV cell on the glass panel, respectively. They can be calculated by ray-tracing method as follows:

$$\alpha_{WPV} = \alpha_{PV}\tau_{PV} + (1 - \tau_{PV}) + \tau_{PV}(1 - \alpha_{PV})(1 - \tau_{PV}), \quad (2)$$

$$\alpha_{NPV} = (1 - \tau) + \tau(1 - \alpha_{wall})(1 - \tau), \quad (3)$$

where α_{PV}, τ_{PV}, τ are the absorptivity of PV cells, the transmissivity of the PV cells' outside layers (glass and EVA1 layers in Fig. 1) and the transmissivity of the elements without PV cell on the glass panel (includes glass, EVA1, EVA2, TPT layers), respectively; E is the electrical power rate generated by PV cells (W/m^2):

$$E = G_{PV}\eta_0[1 - 0.0045(T_p - 25)], \quad (4)$$

where G_{pv} is the solar radiation which arrives on the PV surface through the glass and EVA layers (W/m^2), $G_{PV} = G\tau_{PV}$; η_0 is the electrical efficiency under standard conditions ($1000\,W/m^2$, $25\,^\circ C$), 14% is adopted in this paper.

If the effect of the incident angle θ on the transmissivities is taken into account, a modified coefficient $K_{\tau\alpha}$ is introduced [14]:

$$\tau = \tau_0 K_{\tau\alpha} \quad \tau_{PV} = \tau_{PV0} K_{\tau\alpha},$$

$$K_{\tau\alpha} = 1 - 0.1\left(\frac{1}{\cos\theta} - 1\right), \quad (5)$$

where τ_{PV0}, τ_0 are the transmissivities when incident angle is zero, whose value are 0.81 and 0.6, respectively, if considering the transmissivities of different layers, as well as the PV glass inside and outside surfaces' dirty after more than 1 year's use.

3.2. Energy balance in the air duct

It is assumed that the air temperature in the air duct varies along the vertical direction X only, and then the energy balance in the air duct is as follows:

$$\rho D C_P \frac{dT_a}{dt} = h_{ci}(T_P - T_a) + h_{wo}(T_{wo} - T_a) - \rho V_a D C_P \frac{dT_a}{dX}. \quad (6)$$

The velocity of airflow in the air duct V_a can be calculated as below when the winter air vents are open:

(1) PV-TW without assisted DC fan:

$$V_a = \sqrt{\frac{0.5 \times g\overline{\beta}(T_{out} - T_{in})L}{C_f(L/d) + (C_{in}A_S^2/A_V^2) + (C_{out}A_S^2/A_V^2)}}, \quad (7)$$

$$\overline{\beta} = \frac{1}{\overline{T}} = \left(\frac{T_{in} + T_{out}}{2}\right)^{-1} = \frac{2}{T_{in} + T_{out}}.$$

(2) PV-TW with assisted DC fan:

$$V_a = \sqrt{\frac{0.5 \times g\overline{\beta}(T_{out} - T_{in})L + (\Delta P/\rho)}{C_f(L/d) + (C_{in}A_S^2/A_V^2) + (C_{out}A_S^2/A_V^2)}},$$
$$\Delta P = f(P_f), \quad (8)$$

where d is the duct hydraulic diameter (m), i.e. $d = 2(w+D)$; A_S is the cross-sectional area normal to the height direction of the air duct (m^2), i.e. $A_S = w \times D$; A_V is the area of the winter air vent (m^2); C_f, C_{out}, C_{in} are the friction factor along the air duct, the loss coefficients at the top and bottom vent, respectively; $C_f = 0.3 \times 1.368 \times Gr_x^{0.084}$, $C_{out} = 1.0$, $C_{in} = 1.5$; ΔP is the pressure head provided by DC fan, which is dependent on the instantaneous power of DC fan P_f, and this function is often given by the manufacturer.

3.3. Heat transfer across the southern wall

The southern wall comprises the PV-TW part and the rest part, which is regarded as the normal wall part. It is assumed that the heat transfer across the blackened wall is one-dimensional. The unsteady heat conduction equations and boundary conditions are as follows:

(1) for the PV-TW part:

$$\frac{\partial T_w}{\partial t} = \frac{\lambda_w}{\rho_w C_w}\frac{\partial^2 T_w}{\partial Y^2}, \quad (9)$$

$$-\lambda_w\left(\frac{\partial T_w}{\partial Y}\right)_{y=0} = h_{wo}(T_{wo} - T_a) + \xi_3 h_{rwo}(T_{wo} - T_p) + G\alpha_{wall}\tau_{NPV}(1-\varepsilon),$$
$$-\lambda_w\left(\frac{\partial T_w}{\partial Y}\right)_{y=D_w} = h_{wi}(T_{wi} - \overline{T_r}).$$

(2) for the normal wall part:

$$\frac{\partial T_w}{\partial t} = \frac{\lambda_w}{\rho_w C_w}\frac{\partial^2 T_w}{\partial Y^2},$$

$$-\lambda_w\left(\frac{\partial T_w}{\partial Y}\right)_{y=0} = h_{nwo}(T_{nwo} - T_e) + \xi_1 h_{nrwo}(T_{nwo} - T_e) + G\alpha_{nwall},$$
$$-\lambda_w\left(\frac{\partial T_w}{\partial Y}\right)_{y=D_w} = h_{nwi}(T_{nwi} - \overline{T_r}),$$

where α_{wall}, α_{nwall} are the absorptivities of the blackened wall and normal wall, respectively, ε is the ratio of PV cell coverage.

3.4. Heat transfer in the PV-TW room

The energy balance equation in the room is obtained similar to that in the air duct:

$$\rho C_P L_{room}\frac{dT_r}{dt} = \frac{A_j}{w_{room}L}U_j(T_j - T_r) + R_{Trombe}h_{wi}(T_{wi} - T_r) + (1 - R_{Trombe})h_{nwi}(T_{nwi} - T_r) - \frac{\dot{m}C_P}{w_{room}}\frac{dT_r}{dX}, \quad (10)$$

where $\dot{m}$ is the mass flow rate of the airflow vented from the top winter air vent (kg/s), i.e., $\dot{m} = \rho w D V_a$; R_{Trombe} is the ratio of the PV-TW area to the total southern wall area, i.e. $R_{Trombe} = w/w_{room}$; A_j is the surface area exposed to the interlayer, i.e. the total area of the room wall's surfaces except the southern wall (m^2), $A_j = 2 \times w_{room} \times L_{room} + 2 \times L_{room} \times L + w_{room} \times L$; U_j is the overall heat transfer coefficient between interlayer and indoor room (W/m^2K).

4. Experimental methodology

To test the performance of this system, a comparable hot-box with two rooms, as shown in Fig. 2 (the left room is known as the PV-TW room, and the right one is the

Fig. 2. Graphic representation of the PV-Trombe wall assisted with DC fan and hot-box.

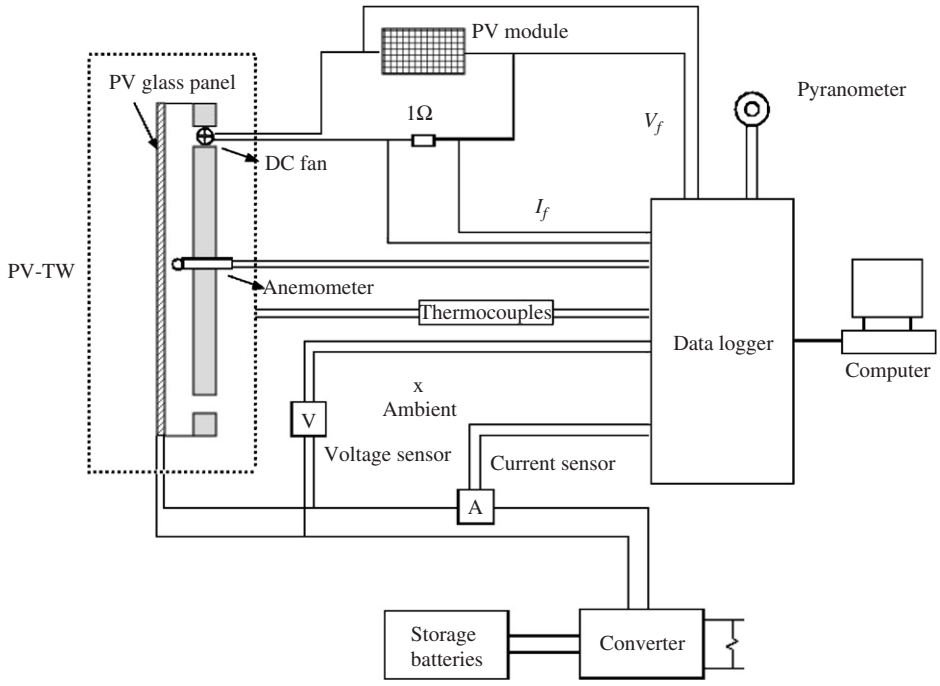

Fig. 3. Scheme of the experimental system.

reference room), was used for performance comparison. Both rooms are of dimensions 2.66 m (height) × 3.00 m (width) × 3.00 m (length) and the room walls' thicknesses are entirely 0.1 m. The PV-TW on the southern wall, which is located at 0.5 m from the western wall, consists of a PV glass panel with an area of 2.66 m (height) × 0.84 m (width) and a thickness of 5 mm, a matt black painted wall and an air duct with a depth of 0.18 m in between. Two winter air vents (0.4 m width × 0.1 m height) are located at 0.07 m from the ceiling and the floor.

A scheme of the experimental system is shown in Fig. 3, and a list of the key apparatus used in the current study is given in Table 1. All measurements were taken within the 4-month period from December 2005 to March 2006 in Hefei. Through the transmission of the performance data via signal wirings to a data acquisition system, the performance of the PV-TW was monitored and recorded all day at every 5 min interval. There were commonly three sunny days at each test trial to illustrate the performance well.

The experimental work reported here focuses on testing the performance of PV-TW under the following two different operation cases:

(1) *Case* 1: PV-TW without assisted DC fan (the original PV-TW);
(2) *Case* 2: PV-TW with assisted DC fan.

Both the two air vents were periodically opened from 9:00 to 17:00, and the DC fan started-up at 9:00 and stalled at 17:00 in the same way.

5. Results and discussions

In order to validate the model by experiments, the measured weather data of Hefei is configured as a data input file of the numerical program based on the model above. The time step is 10 s, the initial time is 1:00 and the initial conditions are initialized according to the measured values at that time. The material properties used in this paper are listed in Table 2 and then the following parameters are obtained to compare the simulated and experimental result: average temperatures of elements with and without PV cell on the glass panel (denoted by T-PB, T-PW, respectively), average air temperature in the air duct (T-A), average temperature of the outside of the blackened southern wall (T-WO), average indoor temperature in the PV-TW room (T-R) and reference room (T-NR), electrical power (P) and efficiency (EFF).

The simulated and experimental results are illustrated in the following figures, where 'S' and 'E' mean the simulated and experimental results; '1' and '2' mean the results in Cases 1 and 2, respectively. After that, the experimental results for Case 1 and Case 2 are compared in order to illuminate the function of the assisted DC fan.

5.1. Case 1: PV-TW without DC fan assisted

When operating in Case 1, the ambient conditions, as shown in Fig. 4, which include G, T_e, T_j and ambient wind velocity (2.0, 3.5 and 2.5 m/s on Decemer 14–16, respectively) are input, and the obtained results are

Table 1
The list of experimental devices

Apparatus	Type	Number	Function	Specification
PV cell	Polycrystalline silicon, 5 cm × 5 cm in size	288	To generate electricity from the captured solar radiation	Area = 0.72 m^2, with 14% light-to-current conversion efficiency at standard conditions, and peak power at 100.8 W_p
Converter	JHQM-102D	1	To convert DC current to AC current	Input 48 V DC current; output 220 V, 50 Hz AC current
Storage battery	Lead-acid battery	4	To store electrical energy	12 V, 65AH, connection in series
Thermocouple	Copper–constantan		To measure temperature	Kept at 0 °C, measured accuracy within ±0.2 °C
Pyranometer	TBQ-2	1	To measure incoming global solar radiation	Kept to the same south-facing vertical surface position as the PV-Trombe wall
Anemometer	EE66-VB5	1	To measure the air velocity in the air duct	
DC fan	WFB1212H	1	To assist PV-TW	12 V, 0.45A
Another PV module		1	To drive the assisted DC fan	10 W_p
Voltage sensor	WBV344S1	1	To measure DC voltage of PV cells	
Current sensor	WBI224S1	1	To measure DC current of PV cells	
Data logger	Agilent 34970A	1	To record measured data	Every 5-min intervals record
Computer	Desktop computer	1	To facilitate data logging	

Table 2
The material properties

Material	Density (kg/m^3)	Specific heat (J/kg K)	Thermal conductivity (W/m K)	Specification
Air	1.18	1000	0.02614	The kinematic viscosity is 1.58×10^{-5} m^2/s
Glass panel	2515	810	1.4	The ratio of PV cell coverage is 0.324, the absorptivity of PV is 0.9
Wall	70	1045	0.026	The absorptivity of the blackened wall and normal wall part is 0.9 and 0.48, respectively

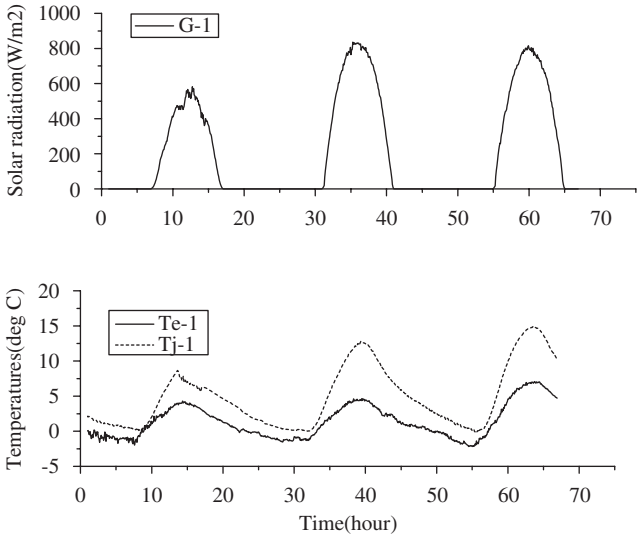

Fig. 4. The ambient conditions on December 14–16, 2005 (Case 1).

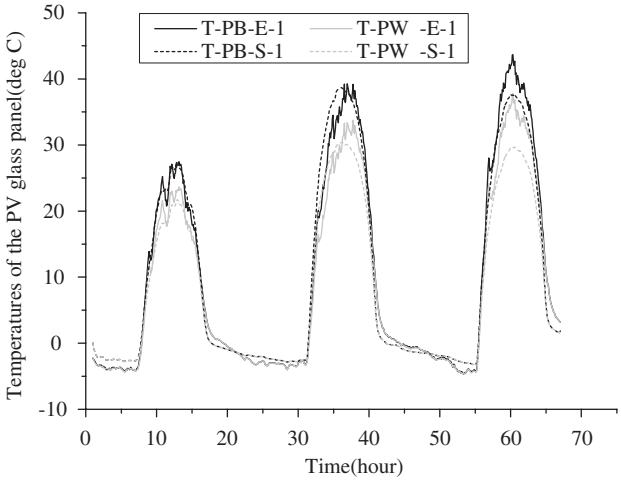

Fig. 5. The temperatures on the PV glass panel in Case 1.

presented as follows:

The 3-day (December 14–16, 2005) temperatures of the PV-TW in Case 1 are shown in Figs. 5–8. It can be seen that most of the simulated results except the average indoor temperature can agree well with the experimental temperatures. It is mainly because that the one-dimensional model of the room is too much simplified to be fit for the case of natural convection. Furthermore, the contrast reflects the

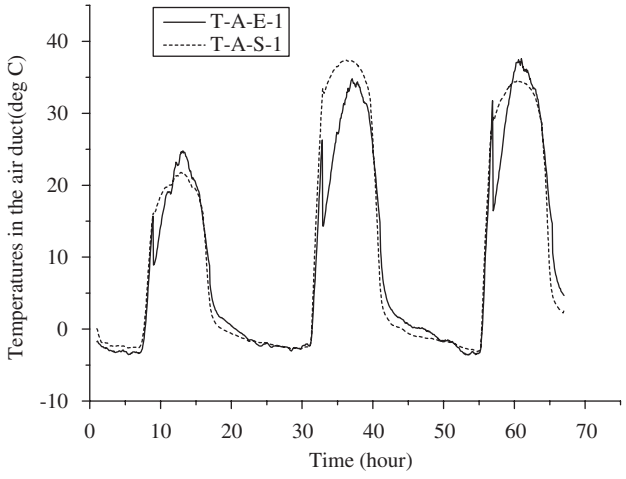

Fig. 6. The temperature in the air duct in Case 1.

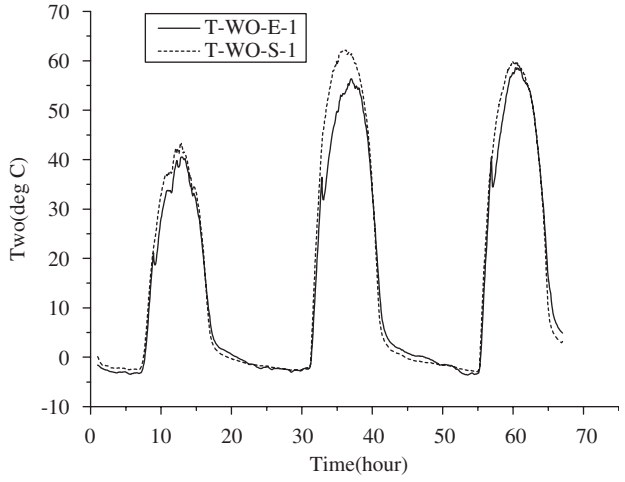

Fig. 7. The temperature of outside surface of PV-TW wall in Case 1.

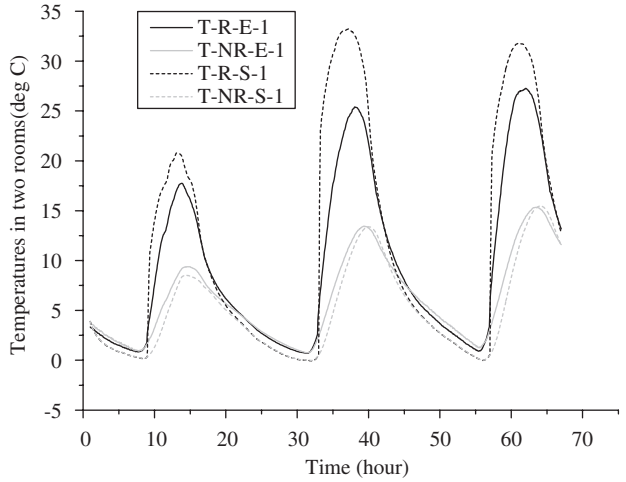

Fig. 8. The temperatures in the two rooms in Case 1.

approximate values taken for thermophysical parameters used in the simulation, the limitation of experimental conditions and the errors of apparatus. Otherwise, from

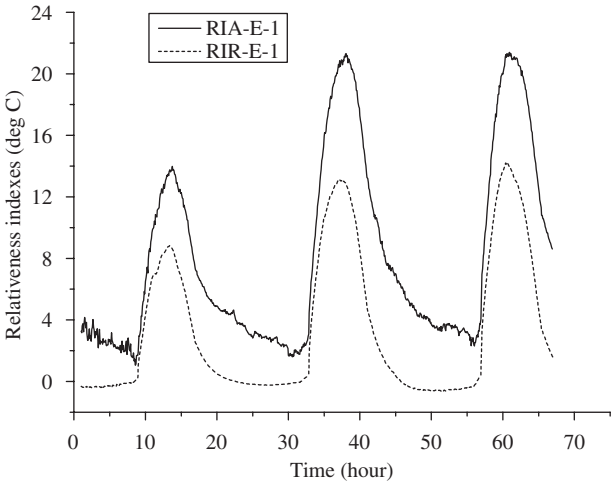

Fig. 9. Relativeness indexes in Case 1.

the four figures above, it should be noticed that the minimum temperatures during 3 days are nearly constant since the minimum ambient temperature only varies a little. This is mainly due to the less thermal capacity of the lightweight laminboard constructed wall and it is so different with that in our former paper [7].

However, based on the more believable field testing results, the analysis of system's performance is conducted and the results are achieved as follows. An important index to evaluate the system's thermal performance is the indoor temperature. A relativeness index, defined as the temperature difference between average indoor temperature and ambient, was introduced [15] as tests would have to be done on different days. Furthermore, due to the use of the comparable hot-box, the indoor temperature difference between the PV-TW room and the reference room is as important as that between indoor room and ambient. Therefore, two different relativeness indexes are defined in this paper, which are denoted by RI-R and RI-A, respectively. As we know, the higher they are, the better system's thermal performance is.

As shown in Fig. 9, the maximum RI-R can reach 14.23 °C while the RI-A can culminate at 21.40 °C, which can be considered to be a significant temperature elevation since the R_{Trombe} is only 0.28.

Unfortunately, the electrical performances during the period (December 14–16, 2005 for Case 1 and December 18–20, 2005 for Case 2) have not been tested as a result of a sudden failure of the converter. However, the electrical performances have been under survey since 2006 and other 2 days (March 13 and March 14, 2006) have been chosen to evaluate the electrical performance for Case 1 and Case 2, respectively.

The daily simulated and experimental electrical power and efficiency are shown in Figs. 10 and 11, respectively. It can be seen the simulated electrical performances can agree well with the experimental results. The statistic of experimental results during the day time (7:00–17:00) shows that the daily periodical average power can reach 30.91 W, with

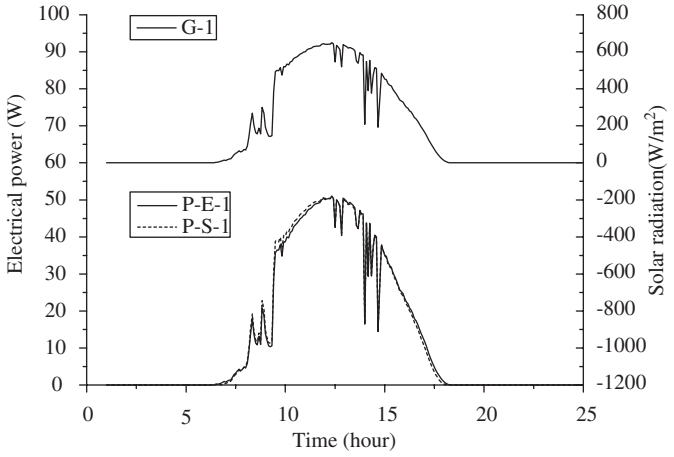

Fig. 10. Electrical power on March 13, 2006 in Case 1.

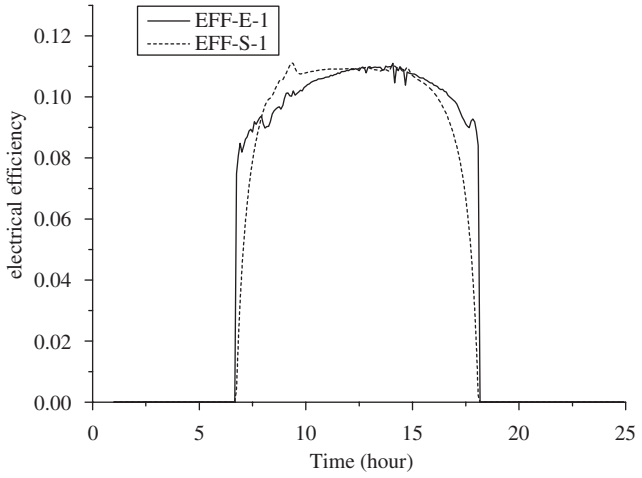

Fig. 11. Electrical efficiency on March 13, 2006 in Case 1.

an average efficiency of 10.61% when the average solar radiation and ambient temperature are 404.63 W/m^2 and 5.47 °C, respectively. It is noticed that the average efficiency is calculated by the equation below, which should describe the ability of generating electricity better:

$$\bar{\eta} = \bar{E}/\bar{G} = \sum E / \sum G. \tag{11}$$

5.2. Case 2: PV-TW assisted with DC fan

When PV-TW is assisted with DC fan, the input of the program should be G, T_e, T_j, wind velocity and the power of the DC fan. However, there was no performance data provided by the manufacturer yet and we decided to do it by ourselves according to our measured data. Then the air velocity in the air duct was fitted into a linear equation as a function of solar radiation:

$$V_a = 0.0822G/100. \tag{12}$$

After that, it replaced Eq. (8) and then was used in the simulation program. At last the simulated results are obtained and shown as below, compared with the experimental results.

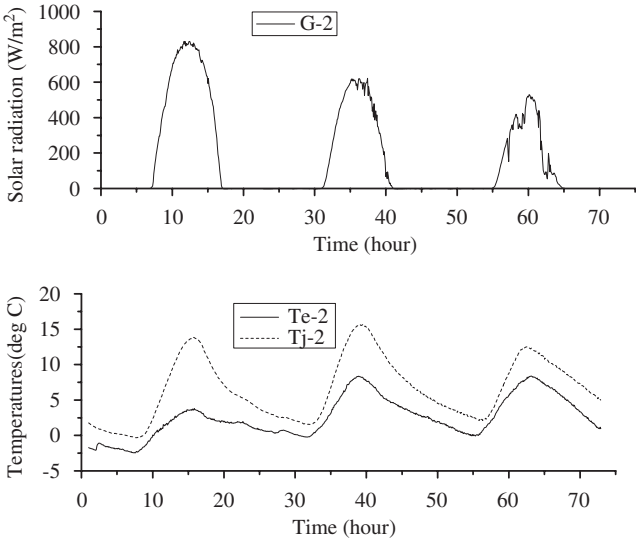

Fig. 12. Ambient conditions on December 18–20, 2005 (Case 2).

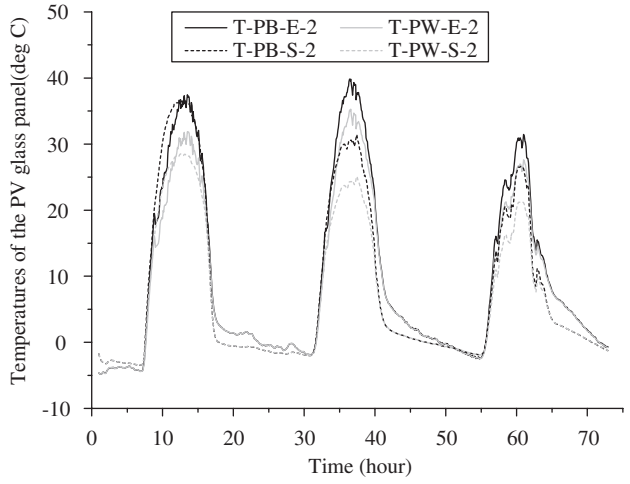

Fig. 13. The temperatures on the PV glass panel in Case 2.

Base on the measured ambient conditions (as shown in Fig. 12, the ambient wind velocities were 3.0, 2.5 and 2.0 m/s on December 18–20, 2005, respectively), the 3-day temperatures of the PV-TW in Case 2 are shown in Figs. 13–16. It can also be seen that the simulated and experimental results can fit considerably well. The differences between simulated and experimental curves can also be explained by the reasons in Section 5.1. The maximum RI-R and RI-A, as shown in Fig. 17, can reach 14.42 and 23.47 °C, respectively.

The simulated and experimental electrical performances are also achieved for another day (March 14, 2006) and found in good agreement, as shown in Figs. 18 and 19. The daily periodical average (during 7:00–17:00) power can reach 33.45 W, with an average efficiency of 10.77% when the average solar radiation and ambient temperature are 431.51 W/m^2 and 10.82 °C, respectively.

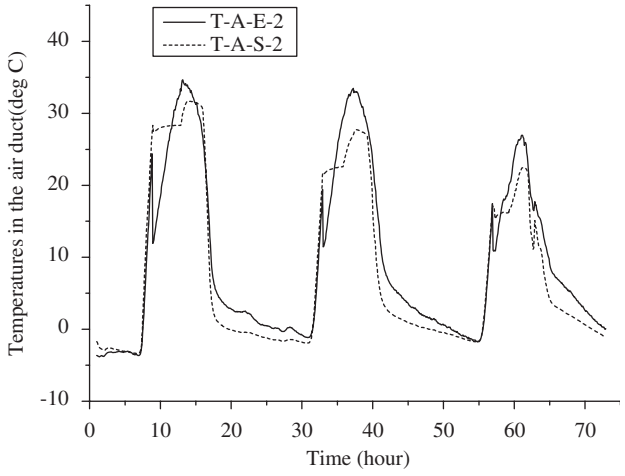

Fig. 14. The temperature in the air duct in Case 2.

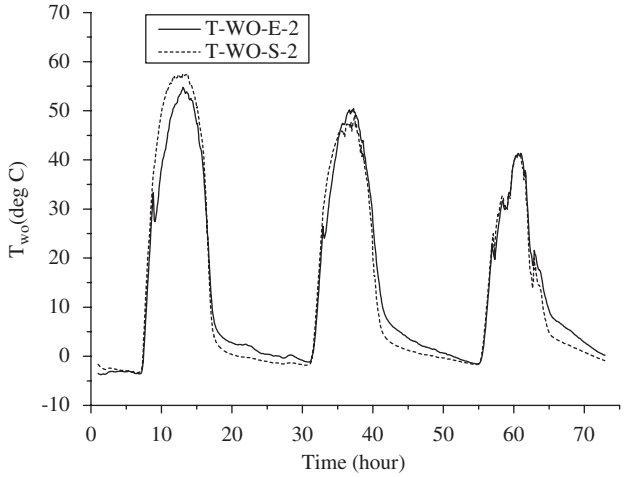

Fig. 15. The temperature of outside surface of PV-TW wall in Case 2.

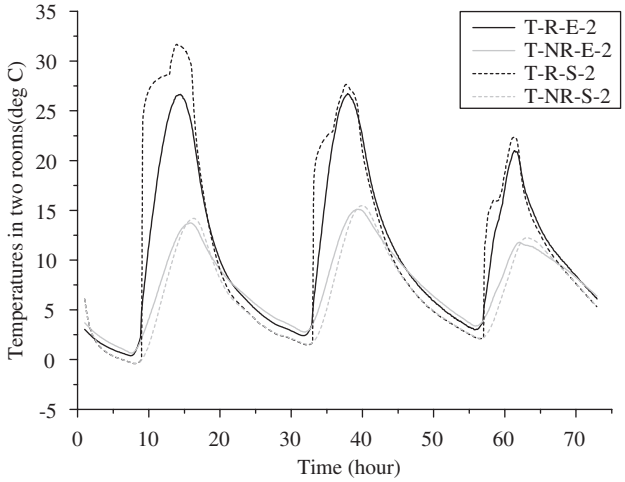

Fig. 16. The temperatures in the two rooms in Case 2.

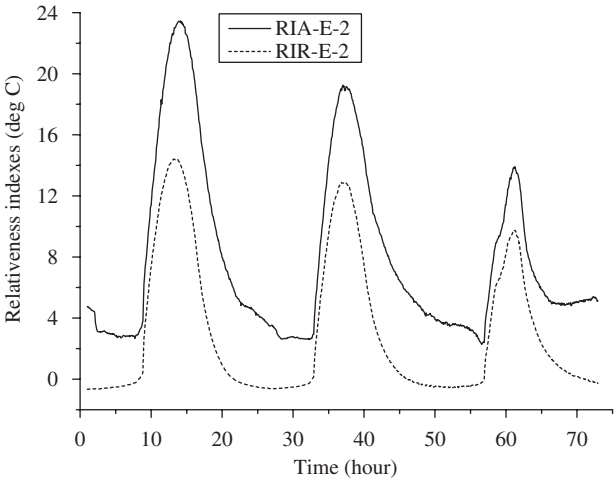

Fig. 17. Relativeness indexes in Case 2.

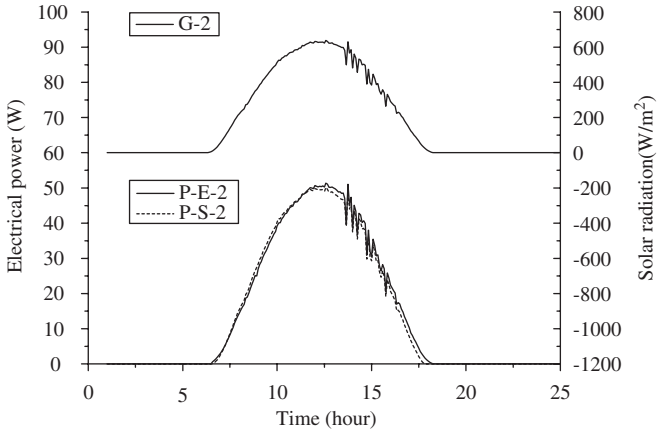

Fig. 18. Electrical power on March 14, 2006 in Case 2.

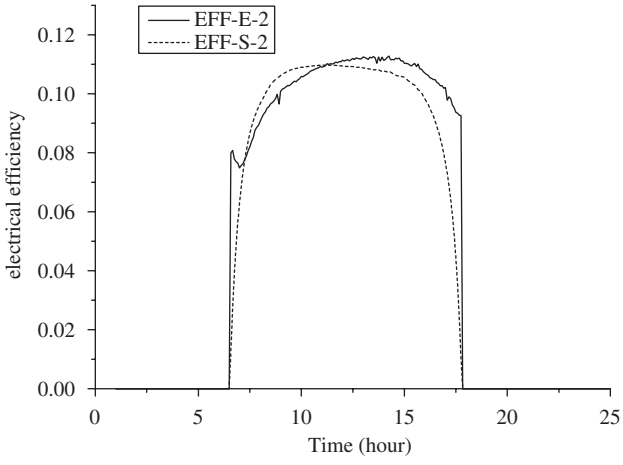

Fig. 19. Electrical efficiency on March 14, 2006 in Case 2.

5.3. Comparison between Case 1 and Case 2

In order to know how DC fan improves the system, the system's performances in these two cases should be

Table 3
The periodical average thermal results during 7:00–17:00 for two cases

Date		Dec. 15(Case 1)	Dec. 18(Case 2)
Measured ambient conditions	G_a(W/m^2)	554.01	557.91
	$T_{e,a}$ (°C)	2.22	1.17
	$T_{j,a}$ (°C)	6.89	7.01
Average thermal results during 7:00–17:00	$T_{pb,a}$ (°C)	25.52	24.24
	$T_{pw,a}$ (°C)	21.63	20.37
	$T_{a,a}$ (°C)	23.89	22.94
	$T_{wo,a}$ (°C)	39.23	37.52
	$T_{r,a}$ (°C)	16.07	16.57
	$T_{nr,a}$ (°C)	8.02	7.83
	RIR_a (°C)	8.05	8.74
	RIA_a (°C)	13.85	15.40

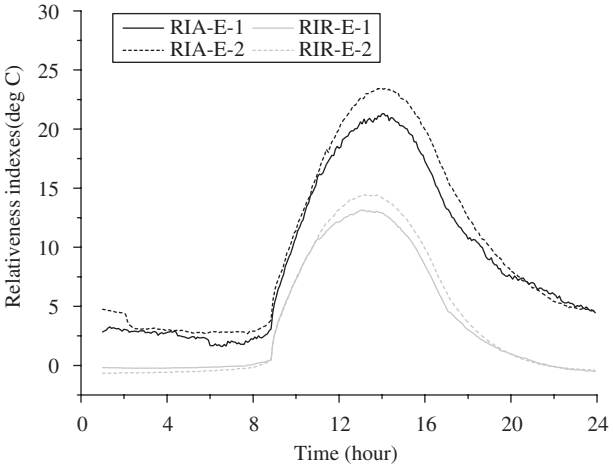

Fig. 20. The comparison of relativeness indexes in two cases.

compared. Nevertheless, experiments in the two cases cannot be carried out at the same time since there is only a PV-TW room. Hence, 2 days (December 15 and 18, 2005) with relatively similar ambient conditions (G, T_e, T_j, and ambient wind velocity) are chosen from our testing trial, and then the periodical average thermal results during day time (7:00–17:00) for two cases are listed in Table 3, in which "a" denotes the periodical average values. It can be observed that, though ambient conditions are not exactly the same, it is demonstrated in the table that the assisted DC fan can help improving the indoor temperature and cooling the PV cells: the average temperature of PV cells reduces by 1.28 °C and the average indoor temperature increases by 0.50 °C. However, the parameters above are dependent on ambient temperature, since the average ambient temperatures on the 2 days are of more than one degree temperature difference. This influence of ambient temperature can be relieved by resorting to the RI-R and RI-A. The relativeness indexes on the 2 days are shown in Fig. 20 and the statistical results show that the average RI-R and RI-A in case 2 increase by 0.69 and 1.55 °C.

Nevertheless, the electrical performances in the 2 days with relatively similar ambient conditions have not been measured, and it is actually difficult to find another 2 days of this kind. Moreover, as can be seen from the electrical results above, the average electrical efficiencies do not distinguish between each other too much, which is due to the further cooling by the assisted DC fan is not big enough, even the measurement errors can exceed the elevated range of the electrical performance. In other words, it does not has to compare the electrical performances, while the PV cells' average temperature reflects this in some sense.

Thus, it is worth using a DC fan to exert the PV-TW system's potential. However, as we can imagine, it is disadvantageous when the DC fan runs too fast due to the considerable heat loss to ambient, so there should be an optimum fan speed. Moreover, its energy consumption should also be underlying consideration, so further theoretical researches and experimental validations are deserved.

6. Conclusion

The objective of this paper is to present a novel improvement of PV-TW: PV-TW assisted with DC fan, and to validate the mathematic model of PV-TW with and without assisted DC fan by field testing results. The simulated and experimental results are found to be in considerably good agreement. A significant temperature increase of indoor temperature with a maximum of 14.42 °C, if compared with the reference room, can be obtained by the PV-TW assisted with DC fan by testing. Meanwhile, the experimental average electrical efficiency of the PV-TW assisted with DC fan can reach 10–11%, due to the glass cover. Furthermore, the experimental results for PV-TW assisted with DC fan show that the average (during 7:00–17:00) temperature of PV cells reduces by 1.28 °C and the average indoor temperature increases by 0.50 °C, while the average RI-R and RI-A increase by 0.69 and 1.55 °C, if compared with the original PV-TW with similar solar radiation, and more than one degree lower ambient temperature. The potential of PV-TW can be exerted in this way.

Nevertheless, some part of the model is too simplified to match the testing results, so an expanding model and some new way of solution will be required. There are also problems such as the optimum fan speed, the fan's energy consumption, which deserve further researches.

Acknowledgements

The study was sponsored by

(1) National Science Foundation of China (NSFC), Project no. 50408009.

(2) Research Center for Photovoltaic System Engineering, Ministry of Education, China.

References

[1] Gan G. A parametric study of Trombe walls for passive cooling of buildings. Energy and buildings 1998;27(1):37–43.
[2] Zrikem Z, Bilgen E. Theoretical study of a compositive Trombe-Michel wall solar collector system. Solar Energy 1987;39(5):409–19.
[3] Zalewski L, Chantant M. Experimental thermal study of a solar wall of composite type. Energy and Buildings 1997;25:7–18.
[4] Raman P, Mande S, Kishore VVN. A passive solar system for thermal comfort conditioning of building in composite climates. Solar Energy 2001;70(4):319–29.
[5] Wei H, Jie J, Aifeng Z, Gang P, Jun D, Hongbo C. Experimental test and data analyze of thermal performance of a solar house with improved Trombe wall. Journal of university of science and technology of China 2003;33(5):567–72.
[6] Benemann J, Chehab O, Schaar-Gabriel E. Building-integrated PV modules. Solar Energy Materials and Solar Cells 2001;67:345–54.
[7] Jie J, Hua Y, Wei H, Gang P, Jianping L, Bin J. Modeling of a novel Trombe wall with PV cells. Building and Environment 2005, in press, doi:10.1016/j.buildenv.2006.01.005.
[8] Hirunlabh J, Wachirapuwadon S, Pratinthong N, Khedari J. New configurations of a roof solar collector maximizing natural ventilation. Building and Environment 2001;36(3):383–91.
[9] Khedari J, Ingkawanich S, Waewsak J, Hirunlabh J. A PV system enhanced the performance of roof solar collector. Building and Environment 2002;37(12):1317–20.
[10] Khedaria J, Waewsak J, Supheng W, Hirunlabh J. Experimental investigation of performance of a multi-purpose PV-slat window. Solar Energy Materials and Solar Cells 2004;82(3):431–45.
[11] Khedari J, Rachapradit N, Hirunlabh J. Field study of performance of solar chimney with air-conditioned building. Energy 2003;28(11):1099–114.
[12] Maneewan S, Khedari J, Zeghmati B, Hirunlabh J, Eakburanawat J. Investigation on generated power of thermoelectric roof solar collector. Renewable Energy 2004;29(5):743–52.
[13] Maneewan S, Hirunlabh J, Khedari J, Zeghmati B, Teekasap S. Heat gain reduction by means of thermoelectric roof solar collector. Solar Energy 2005;78(4):495–503.
[14] Duffie JA, Beckman WA. Solar engineering of thermal processes, second ed. New York: Wiley; 1991.
[15] Khedari J, Boonsri B, Hirunlabh J. Ventilation impact of a solar chimney on indoor temperature fluctuation and air change in a school building. Energy and Building 2000;32:89–93.